From Human MRI to Microscopy: Co-registration of Human Brain Images to Postmortem Histological Sections

M. Singh, *Senior Member, IEEE,* A. Rajagopalan, C. Zarow, X.-L. Zhang, T.-S. Kim, D. Hwang, A.-Y. Lee, H. Chui

***Abstract*– Small vascular lesions seen in human MRI are detected reliably only in postmortem histological samples. Using non-linear Polynomial transformation, we report a method to co-register in-vivo MRIs to microscopic examinations of histological samples drawn off the postmortem brain. Digital photographs of postmortem slices served as an intermediate reference to co-register the MRIs to microscopy. In-vivo MRI to postmortem co-registration is challenging due to gross structural deformations in the brain during extraction. Hemispheres of the brain were co-registered separately to mitigate these effects. Approaches relying on matching single-slices, multiple-slices and entire volume in conjunction with different similarity measures suggested that using four slices at a time in combination with two sequential measures, Pearson correlation coefficient followed by mutual information produced the best MRI-postmortem co-registration according to a voxel mismatch count. The accuracy of the overall registration was evaluated by measuring the 3D Euclidean distance between the locations of the microscopically identified vascular lesions and their MRI-postmortem co-registered locations. The results show a mean 3D displacement of 7.5 ± 2.7 mm between these locations for 11 vascular lesions in 7 subjects.**

I. INTRODUCTION

A microscopic examination of histological samples is often the gold-standard to detect pathology. For example, in diseases such as Alzheimer Disease or Vascular Dementia, small lesions may be visualized during *in-vivo* MRIs, but are detected reliably only at postmortem. With the objective of improving the detection and characterization of such small lesions seen in human MRIs but ascertained only at postmortem, we have developed a method to co-register MRI visualized lesions to those detected by a microscopic examination of histological samples drawn off the postmortem brain. The approach relies upon co-registration of digital photographs of the postmortem brain to the *in-vivo* MRI of the person when he or she was alive and mapping suspected lesions from the MRI to the corresponding postmortem slice. Relying on this image-guided procedure, samples are then drawn from a small region surrounding the location of mapped lesions in the postmortem slice, stained and examined microscopically to identify lesions. The locations of the microscopically detected lesions are marked on the histological samples. These marked samples are then co-registered back onto the postmortem slice. Thus the postmortem brain slices become the common frame-of-reference onto which the in-vivo MRI and the histological exam are mapped to achieve co-registration between MRI and microscopy.

Previous work to co-register in-vivo MRIs to microscopically examined samples has been reported mostly for small animals [1-4], a limited number of primates [5] and relatively few human studies [6-8]. Animal studies have an advantage over human studies in that animals can be sacrificed immediately after an in-vivo scan, the postmortem brain can also be scanned, and then the postmortem brain can be frozen and sliced for a microscopic histological examination. Thus very little time elapses between the in-vivo, postmortem and microscopic examinations, thereby minimizing changes in the shape and structure of the brain viewed by the different modalities. Also, in animal studies it is logistically straightforward to obtain a scan of the premortem and postmortem brain. Thus a MRI of the postmortem brain is available to co-register with the microscopic examination.

In human studies, however, frequently there is a large time-gap, on the order of 1-3 years, between the in-vivo MRIs and when the person comes to postmortem. Also logistically it is difficult to arrange for a MRI of the postmortem brain, and in the work reported here, no MRIs of the postmortem brain were available. Give these practical constraints, the objective of this work was to co-register in-vivo MRIs to digital photographs of postmortem slices and subsequent histological sections under the assumption that only in-vivo MRIs (which may have been done several years prior to death) are available, and that no postmortem MRIs would be available. Postmortem images in this paper specifically refer to digital photographs of the sliced postmortem brain and not any postmortem MRIs.

Co-registering these photographs of the postmortem slices to corresponding in-vivo MR slices is a challenging task for a number of reasons: 1) The time lapse between the in-vivo MRI and the postmortem brain creates structural discrepancy, 2) the procedure to extract the brain from the cranial vault leads to multiple deformations such as collapse of the

Manuscript received November 17, 2006. This work was supported in part by NIH Grants NIA-NIH 1PO1AG 12453 and NIA-NIH P50 AG05142.

M. Singh. A. Rajagopalan, and D. Hwang are with the Departments of Radiology and Biomedical Engineering, University of Southern California, Los Angels, California, USA (Contact author e-mail: msingh@usc.edu).

C. Zarow, X.-L. Zhang, A.-Y. Lee and H. Chui are with the Department of Neurology, University of Southern California, Los Angels, California, USA. T. S. Kim was with the Departments of Radiology and Biomedical Engineering, University of Southern California, Los Angels, California, USA. He is now with the Department of Biomedical Engineering, College of Electronics and Information, Kyung Hee University, Kyungki, South Korea.

ventricles and other regions, distortions while slicing, and deformations due to dehydration, and 3) the variability in the thickness and orientation of the postmortem brain slices makes dense 3D-volume reconstruction of the postmortem brain difficult.

Current image registration approaches perform efficiently if evenly sliced and orientation-preserved slices are available such that an accurate 3D reconstruction of the image volume is possible. The application of these existing registration methods to the problem at hand is severely limited by the difficulty in forming an accurate 3D-volume of the postmortem photographic images due to significant interslice gaps and severe geometrical distortions. The registration task becomes more challenging due to pixel-voxel size mis-match, scaling, global and local geometrical distortions and regions present in one but missing from the other modality.

The method reported here relies on registering multiple postmortem slices to a warped 3D space within the MRI volume. Warping relies on a modified n^{th}-order non-linear polynomial approach developed by one of us to co-register Thallium stress heart images to resting images in nuclear medicine [9]. Eight different voxel similarity measures were evaluated based on a pixel mismatch count to derive an optimal similarity measure comprising a combination of two similarity measures. The overall registration methodology was evaluated by identifying specific vascular lesions called lacunes (irregular cavities containing strands of fibrillar connective tissue) in brain MRIs of patients diagnosed with vascular dementia, mapping suspected lesions from the MRI to the corresponding postmortem slice, drawing histological samples from the region surrounding the mapped lesions in the postmortem slice, examining these samples microscopically to identify lesions, marking the locations of the lesions seen microscopically and co-registering these marked spots back onto the postmortem brain. Details of the registration methodology and results showing a relatively good match between the locations of lesions obtained from the MRI-postmortem co-registration and their microscopically verified locations are presented in this paper.

II. METHOD

Specimens of postmortem brains were fixed in 10% neutral formalin for at least two weeks, and sectioned into 25-30 5mm thick coronal slices using a motor-driven rotary slicer. Each slice was then photographed digitally and stored in Kodak PhotoCD RGB color format at a resolution of 3072x2048, keeping an in-plane spatial resolution of approximately 0.6mm. The brain was extracted from the background of the RGB postmortem photographs by selectively thresholding RGB intensity values and converted to gray-scale by eliminating the hue and saturation while retaining the luminance information. In handling the postmortem brain, maintaining a relative distance between two hemispheres is difficult, since only the corpus callosum connects the hemispheres. Thus we separated the brain into hemispheres by slicing through the corpus callosum and registered each hemisphere separately. To minimize distortions due to mechanical slicing and dehydration, and to reduce the variability in the planar thickness and orientation of the postmortem slices, each hemisphere was embedded in 5% agar gel and a set of coronal brain slices was obtained as shown in Fig. 1. A 3D volume was reconstructed from these coronal slices after aligning them to each other with the help of six fiducial markers arranged in two columns (see Fig 1). More details of this standardized procedure for gel-embedding and handling the postmortem brain have been reported elsewhere [10].

Fig 1: Digital photograph of the right brain hemisphere of a postmortem slice embedded in gel. The six fiducial markers used in the realignment procedure are also shown on the sides.

Coronal T1-weighted (in-plane resolution 0.86x0.86mm^2, slice-thickness=1.5mm), axial Proton Density (PD), and axial T2-weighted (1.0x1.0 mm^2 in-plane resolution, slice thickness=3mm) MRIs were acquired on a GE 1.5T Signa system. The Brain Surface Extraction (BSE) Algorithm [11], which extracts the brain regions using a morphological algorithm, was used to strip off the skull and scalp in MR images. In addition, the regions of pons and cerebellum were removed manually from each MR slice, since these regions were absent in the postmortem slices. To match the slices of each hemisphere of the postmortem brain, each extracted MR brain volume was also cut into two hemispheres through the inter-hemispheric fissure and stored separately. A 3D MR volume was reconstructed from the acquired coronal slices and coarsely aligned with the postmortem volume using rigid-body rotation.

Multiple postmortem slices were then matched to their corresponding MRI volume by a non-linear Polynomial warping approach [9]. It was found that a single postmortem slice to MRI volume matching approach reported by us previously [12] had limited success and matched only the central portion of the brain. Attempts to co-register the entire postmortem brain simultaneously to the MRI volume also failed due to gross distortions between the two modalities. We have now developed a method where multiple postmortem slices (four in the current work) are co-registered to a small portion of the MRI volume as described in the following.

A modified general n^{th}-order polynomial transformation was used to warp the MRI volume to match each slice within a selected four-slice set of the postmortem images and the procedure was repeated for all sets of postmortem slices. Coordinates were transformed in the following manner [9,12]:

$$\begin{aligned} u &= a_0 + a_1 i + a_2 j + a_3 i^2 + a_4 ij + a_5 j^2 \\ v &= b_0 + b_1 i + b_2 j + b_3 i^2 + b_4 ij + b_5 j^2 \\ w &= c_0 + c_1 i + c_2 j + c_3 i^2 + c_4 ij + c_5 j^2 \end{aligned} \qquad (1)$$

where (u,v,w) are the new coordinates in the 3D MRI, (i,j) are a pixel's coordinates in a postmortem image, and a_i, b_i and c_i are the coordinate transformation coefficients.

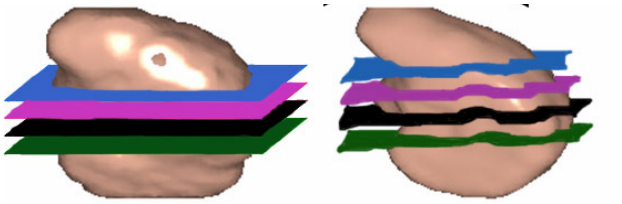

Fig 2: (left) Initial location of four postmortem slices within the MRI volume, and (right) the warped MRI volume matching the postmortem slices.

The set of four slices was first matched approximately to their location in the MRI volume and the MRI volume was then recursively resliced around the calculated location to maximize a similarity measure or minimize a cost-function to estimate the coefficients a_i, b_i and c_i. The procedure is schematically shown in **Fig. 2** where the position of the four slices is shown at the left and the warped MRI volume matching these slices is shown at the right.

Eight different similarity measures described previously [13], were evaluated in terms of a voxel mismatch count [14], leading to a two-step approach where geometrical distortions were corrected in a first step by Pearson cross-correlation (which matched the size and shape of the brain) followed by mutual information maximization to match internal structures and intensity distribution. Specifically, the cross correlation was calculated at every iteration and iterations continued till it was maximized and the resulting parameters were used as initial guesses for the next set of iterations where the mutual information was maximized.

The co-registration procedure was evaluated by measuring the error between microscopically identified vascular lesions drawn off the postmortem slices and the locations of the presumably same lesions in MRIs of the same person when he/she was alive. These vascular lesions were best identified in the axial scans (PD and T2 weighted images). An expert marked the locations of these lesions. These locations were first mapped from axial to coronal sections by volume reslicing and then mapped onto the postmortem slices by using the Polynomial-transformation parameters found by the warping technique described above.

Relatively large samples of the postmortem slices around these marks were then extracted and sent to a pathologist for stained microscopy. The pathologist sub-sliced the samples into 10-20 micron sections and through a microscopic examination, marked the regions where these lesions were identified histologically. Microscopy pictures were generated at several magnifications. Frequently portions of the sample disintegrated during the staining and sub-slicing procedures. Thus another warping procedure was required to co-register the microscopy pictures back to the postmortem slices.

Co-registration of the microscopy pictures to corresponding postmortem slices was also accomplished by warping the microscopy pictures using a second order Polynomial coordinate transformation presented in eq (1). An edge-matching cost-function was used which minimized the pixel mismatch count between the intact edges of the microscopy image and edges in the postmortem image at corresponding boundaries. Since the regions from where the samples were extracted for microscopic examination were known, it was not difficult to initially start with a rough alignment of the intact boundaries in the microscopy images to corresponding boundaries in the postmortem slices. The missing boundaries were then masked and alignment was refined iteratively by the warping procedure. The accuracy of the entire procedure to co-register in-vivo MRI to microscopic findings was evaluated by quantifying the displacement between a) the locations of in-vivo MRI detected lesions mapped onto a postmortem slice and b) the location of presumably the same lesion identified through a microscopic examination and then co-registered back to its corresponding postmortem slice. Since the MRI marked lesions extended over several slices, the 3D coordinates of the centroid were used to compute the displacement. However, since the microscopic examinations were performed on 10-20 micron thick sections peeled off a 5mm thick postmortem slice, the 3D coordinates corresponding to the middle layer of the postmortem slice were used in the displacement computation.

III. RESULTS

The complete MRI to microscopy co-registration was carried out for 16 lesions detected in seven subjects. An example of the MRI to postmortem registration is shown in **Fig. 3.** The postmortem slices are shown in the top row and the co-registered MRI slices are shown in the bottom row. It is clear that there is strong match in the size, shape, and internal structures including outer and inner contours of the ventricles, subcortical grey nuclei, hippocampus, gyri, and sulci. Two examples of the entire MR to microscopy procedure are presented in **Figs 4 and 5**. The locations of the lesions marked on axial T2 images by an expert are shown in Figs. 4-5(a). These lesions were transferred to the postmortem slices through co-registration. As an example, the locations of the lesions in one hemisphere are shown in Figs. 4-5(b). Their locations in corresponding warped MRI sections are shown in Figs. 4-5(c). Figs. 4-5(d) show the locations of the histology slides after warping boundaries in the stained sections to match their original boundaries in the postmortem brain.

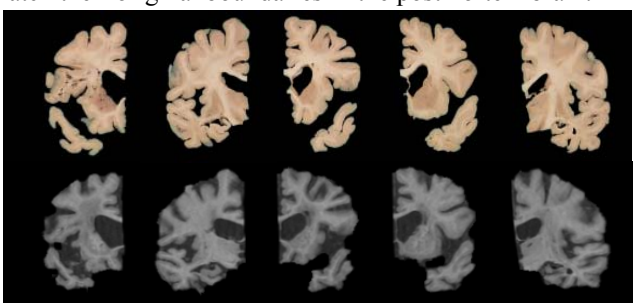

Fig 3: (top row) Postmortem slices (digital photographs). As an example, two slices from the left hemisphere and three slices from the right hemisphere are shown. (bottom row) Co-registered MRI slices obtained from a warping of the MRI volume.

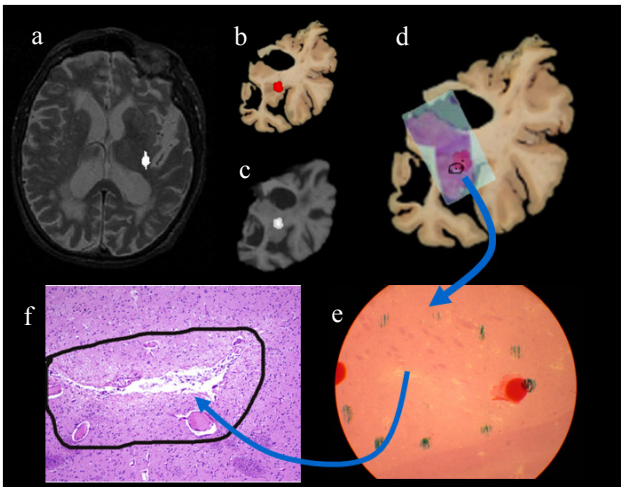

Fig 4: (a) lesion marked on T2 scan, (b-c) co-registered postmortem and MRI sections with lesion location, (d) postmortem slice with co-registered histological section, (e) area identified to contain a lesion at histology (coarse microscopy), (f) Microscopic details of the identified area showing details of the lesion.

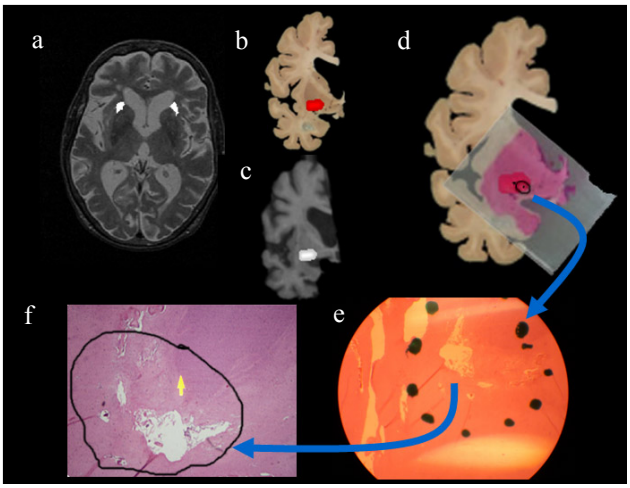

Fig 5: Same as in Fig. 4 for a different subject

The black circles with a dot at the center correspond to the locations of the lesions identified through the microscopic examination of the histology slides. The red areas are the locations of the lesions through MRI-postmortem co-registration. Areas identified to contain a lesion during histology at a coarse microscopic resolution are shown in Figs 4-5(e), and high magnification microscopy images of the lesions within this region are shown in (f). The dots within the black circle in Figs. 4-5(d) correspond to the microscopic locations of the respective lesions. The 3D displacements between the microscopic locations and the centroids of the same lesions identified through MRI-postmortem co-registration are shown in Table I.

IV. CONCLUSION

We have developed a technique to co-register human in-vivo MRIs to microscopic images of targeted regions at postmortem. The approach relies on using digital photographs of postmortem slices as a reference upon which the in-vivo MRIs and microscopic histological exams are co-registered. The accuracy of the procedure was evaluated by computing the displacement between the in-vivo MRI identified lesions to their corresponding locations determined by a microscopic exam of histological sections in postmortem brain slices. Results reveal that the co-registration identifies the locations of 11 lesions in 7 subjects within an error of 7.5 +/-2.7 mm.

Case No	3D Euclidean dist.(cm)
1	0.928
	0.871
2	0.492
	0.472
3	1.099
	1.071
4	0.423
5	0.348
6	0.759
	0.855
7	0.91
Average	0.748
Std dev. =	0.268

Table 1: The 3D Euclidean distances between the centroids of lesions identified by MRI to postmortem co-registration and by microscopy.

REFERENCES

[1] M.A. Jacobs et al. "Registration and warping of magnetic resonance images to histological sections", *Med Phys* **26(8)**:1568-1578, 1999.

[2] Y. Jiang et al. "Three-dimensional diffusion tensor microscopy of fixed mouse hearts", *Magn Reson Med* **52**:453-460, 2004.

[3] C.R. Meyer et al. "A methodology for registration of a histological slide and in-vivo MRI volume based on optimizing mutual information", *Mol Imaging* **5(1)**:16-25, 2006.

[4] A.W. Anderson et al. "Comparison of brain white matter fiber orientation measurements based on diffusion tensor imaging and light microscopy", *Proc. 28-th IEEE EMBS Conf.* 2006.

[5] J.A. Kaufman et al. "Anatomical analysis of an Aye-Aye brain combining histology, structural magnetic resonance imaging, and diffusion tensor imaging", *Anatomical Record*, **287A**:1026-1037, 2005.

[6] T. Schormann et al. "Statistics of deformation in histology and application to improved alignment with MRI", *IEEE Trans Med Img* **14(1)**: 25-35, 1995.

[7] M.S. Mega et al. "mapping histology to *metabolism*; Coregistration of stained whole-brain sections to premortem PET in Alzheimer's Disease", NeuroImage **5**:147-153, 1997.

[8] C. Kenwright et al. "2-D to 3-D refinement of postmortem optical and MRI co-registration", *MICCAI*, LNCS **2879:**935-944, 2003.

[9] M. Singh et al. "A digital technique for accurate change detection in nuclear medicine images with applications to myocardial perfusion studies using thallium-201", *IEEE Trans Nucl Sci* **26**: 565-575, 1979.

[10] C. Zarow et al. "A standarized method for brain cutting suitable for both stereology and MRI-brain coregistration. J Neurosci Meth **139(2)**:209-215, 2004.

[11] S. Sandor and R. Leahy, "Surface-Based labeling of cortical anatomy using a deformable atlas", *IEEE Trans Med Img* **16(1)**: 41-54, 1997.

[12] T.S. Kim et al. "Automatic registration of postmortem brain slices to MRI reference volume. *IEEE Trans Nucl Sci* **47(4)**:1607-1613, 2000.

[13] M. Holden et al. "Pixel similarity measures for 3-D serial MR brain image registration", *IEEE Trans Med Imag* **19(2)**:94-102, 2000.

[14] P.A. Freeborough et al. "Accurate registration of serial 3D MR brain images and its application to visualizing change in neurodegenerative disorders. *J Comp Assisted Tomogr* **20(6)**:1012-1022, 1996.